JOC Article
pubs.acs.org/joc

Binding of Carboxylic Acids by Fluorescent Pyridyl Ureas

Lisa M. Jordan,[†] Paul D. Boyle,[‡] Andrew L. Sargent,*[,†] and William E. Allen*[,†]

[†]*Department of Chemistry, Science and Technology Building, East Carolina University, Greenville, North Carolina 27858-4353, United States, and* [‡]*Department of Chemistry, North Carolina State University, Raleigh, North Carolina 27695-8204, United States*

allenwi@ecu.edu; sargenta@ecu.edu

Received September 2, 2010

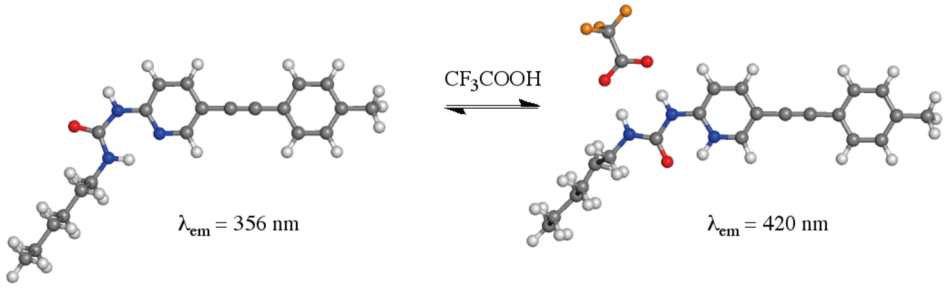

Fluorescent pyrid-2-yl ureas were prepared by treating halogenated 2-aminopyridines with hexyl isocyanate, followed by Sonogashira coupling with arylacetylenes. The sensors emit light of ~360 nm with quantum yields of 0.05−0.1 in acetonitrile solution. Addition of strong organic acids (pK_a < 13 in CH_3CN) shifts the fluorescence band to lower energy, and clean isoemissive behavior is observed. Fluorescence response curves (i.e., F/F_0 vs $[acid]_{total}$) are hyperbolic in shape for CCl_3COOH and CF_3COOH, with association constants on the order of 10^3 M^{-1} for both acids. ^1H NMR titrations and DFT analyses indicate that trihaloacetic acids bind in ionized form to the receptors. Pyridine protonation disrupts an intramolecular H-bond, thereby unfolding an array of ureido N*H* donors for recognition of the corresponding carboxylates. Methanesulfonic acid protonates the sensors, but no evidence for conjugate base binding at the urea moiety is found by NMR. An isosteric control compound that lacks an integrated pyridine does not undergo significant fluorescence changes upon acidification.

Introduction

Recognition of carboxylic acids is complicated by their potential to dissociate. Indicator compounds rely upon such behavior, changing color in response to the hydrogen ions so generated, yet they do not typically feature designated sites for binding of the corresponding conjugate bases. Pyrid-2-yl ureas and thioureas are suitable platforms for the development of acid receptors, as their conformational flexibility allows them to recognize the ionized or molecular forms of RCOOH. In organic solution, pyridyl ureas adopt a folded shape in which one of the ureido NH groups is intramolecularly hydrogen bonded to the heterocyclic N atom.[1] Strong acids such as CF_3COOH or HBF_4 protonate the pyridine ring,[2] causing the (thio)urea moiety to change orientation and present two *syn* NH groups suitable for anion binding.[3] Acids that are too weak to protonate the base do not bring about conformational switching, and are recognized in their undissociated state at the peripheral NH and CO units.[4] For this work, pyridyl ureas were incorporated into diarylacetylene reporter units[5] to generate a series of functional fluorophores. The response of the sensors to a series of organic acids

(1) (a) McGhee, A. M.; Kilner, C.; Wilson, A. J. *Chem. Commun.* **2008**, 344–346. (b) Chien, C.-H.; Leung, M.-K.; Su, J.-K.; Li, G.-H.; Liu, Y.-H.; Wang, Y. *J. Org. Chem.* **2004**, *69*, 1866–1871. (c) Corbin, P. S.; Zimmerman, S. C.; Thiessen, P. A.; Hawryluk, N. A.; Murray, T. J. *J. Am. Chem. Soc.* **2001**, *123*, 10475–10488.

(2) Rashdan, S.; Light, M. E.; Kilburn, J. D. *Chem. Commun.* **2006**, 4578–4580.

(3) (a) Carroll, C. N.; Berryman, O. B.; Johnson, C. A.; Zakharov, L. N.; Haley, M. M.; Johnson, D. W. *Chem. Commun.* **2009**, 2520–2522. (b) Byrne, P.; Lloyd, G. O.; Clarke, N.; Steed, J. W. *Angew. Chem., Int. Ed.* **2008**, *47*, 5761–5764. (c) Catalgirone, C.; Bates, G. W.; Gale, P. A.; Light, M. E. *Chem. Commun.* **2008**, 61–63. (d) Custelcean, R.; Jiang, D.; Hay, B. P.; Luo, W.; Gu, B. *Cryst. Growth Des.* **2008**, *8*, 1909–1915. (e) Ghosh, K.; Masanta, G.; Chattopadhyay, A. P. *Tetrahedron Lett.* **2007**, *48*, 6129–6132.

(4) Goswami, S.; Jana, S.; Dey, S.; Sen, D.; Fun, H.-K.; Chantrapromma, S. *Tetrahedron* **2008**, *64*, 6426–6433.

(5) (a) Jo, J.; Lee, D. *J. Am. Chem. Soc.* **2009**, *131*, 16283–16291. (b) Yamaguchi, Y.; Shimoi, Y.; Ochi, T.; Wakamiya, T.; Matsubara, Y.; Yoshida, Z. *J. Phys. Chem. A* **2008**, *112*, 5074–5084. (c) Wong, J.; Masson, P.; Nicoud, J.-F. *Polym. Bull.* **1994**, *32*, 265–272.

Published on Web 11/16/2010 DOI: 10.1021/jo101730w

SCHEME 1

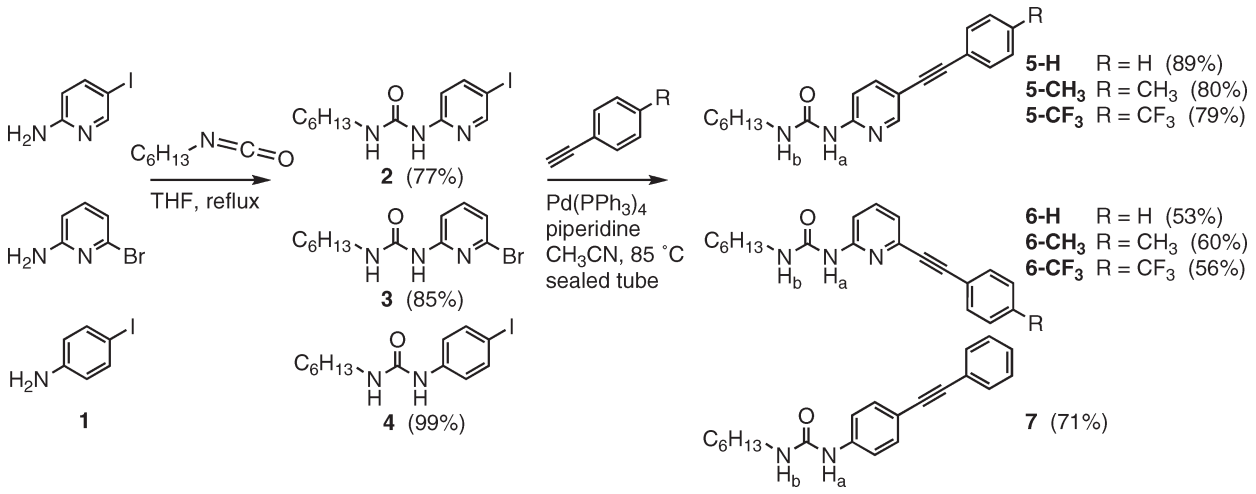

was evaluated in acetonitrile solution, where the extent of acid ionization is low.

Results and Discussion

Synthesis and Structure of the Sensors. The desired fluorophores were prepared on a ~0.5 g scale in two steps without chromatographic purification (Scheme 1). Commercially available halogenated arylamines **1** were treated with hexyl isocyanate in THF at reflux to afford crude ureas **2**−**4**. These intermediates were purified by washing CH_2Cl_2 solutions with 5% HCl to remove unreacted amines. Using a modular approach to impart electronic variability in the fluorophore, substituted ethynylarenes were coupled to **2**−**4** under Cu-free Sonogashira conditions to provide the isomeric sets of products **5** and **6**,[6] and nonpyridinic control compound **7**. In all cases, analytically pure materials crystallized out of the reaction mixtures upon cooling.

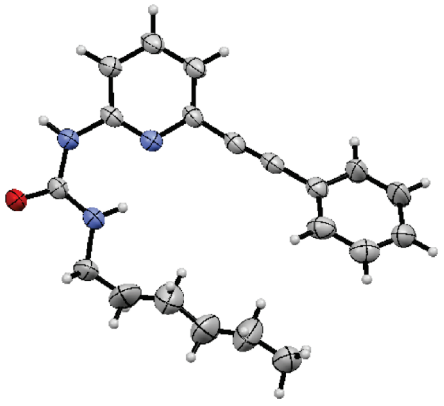

FIGURE 1. View of **6-H** in the crystal. Thermal ellipsoids are scaled to the 30% probability level.

Crystals of **6-H** suitable for X-ray diffraction were grown from acetonitrile in the absence of acids. Figure 1 shows one of the two crystallographically independent molecules found in the unit cell. The sensor adopts a compact, hairpin-like conformation stabilized by an intramolecular hydrogen bond involving H_b ($N_{ureido}\cdots N_{pyridyl}$ = 2.70 Å). Close approach between the hexyl chain and the phenyl group, presumably resulting from packing forces, is accompanied by rotation of the ring by 32° relative to the plane defined by the pyridine heterocycle. Molecules of **6-H** are further organized into dimers via pairs of H-bonds at the external NH_a and CO units.[1c,4] The hydrogen bonding present in solid samples of **6-H**/**CH_3**/**CF_3** is stronger than that of the 5-isomers, as judged by IR stretching frequencies of the NH groups. Comparing **6-H** to **5-H**, for example, the former has H-bonded NH-stretches at 3214 and 3122 cm^{-1}, while the latter's appear at 3224 and 3134 cm^{-1}.

In acetonitrile solution, the proton NMR chemical shifts of ureido proton H_b in **5-H**/**CH_3**/**CF_3** (8.35, 8.35, and 8.30 ppm, respectively) and **6-H**/**CH_3**/**CF_3** (8.54, 8.58, and 8.46 ppm) indicate that the sensors retain a folded conformation that is not available to control compound **7** (δ_{Hb} = 5.23 ppm). Previous work with 1-butyl-3-(4-methylpyridin-2-yl)urea has established the shift of this resonance to be concentration-independent in $CDCl_3$.[1c] In CD_3CN, no changes in δ_{Hb} occurred as a solution of **6-H** was diluted from 2.1×10^{-3} M to 9.0×10^{-5} M. Taken together, the NMR and IR data are consistent with the closed forms of the 6-arylethynyl isomers being marginally more stable than those with 5-substitution. Heating disrupts the intramolecular H-bonding to a small extent. When a 6.02×10^{-3} M solution of **5-H** in CD_3CN was warmed from 50 to 90 °C in a flame-sealed tube, the H_b signal moved upfield by 0.2 ppm.

Fluorescence Response to Acids. In the absence of acids, sensors **5**−**6** show a single featureless fluorescence band between 350 and 370 nm in N_2-saturated acetonitrile (Table 1). Fluorescence quantum yields (Φ_F) for electron-rich systems **5-H**/**CH_3** and **6-H**/**CH_3** are higher than those of the trifluoromethyl-substituted analogues. Incremental addition of trichloroacetic acid (pK_a in CH_3CN = 10.75[7]) or trifluoroacetic acid (12.65) causes bathochromic shifts of 49 and 64 nm in the emission profiles of **5-H** and **5-CH_3**, respectively (Figure 2a), with modest drops in Φ_F that qualitatively obey the energy gap law.[8]

(6) Compound numbers in Scheme 1 were assigned so that sensors with arylacetylene units attached to position 5 of the pyridine ring begin with "**5**", and those featuring C-6 substitution begin with "**6**".

(7) (a) Eckert, F.; Leito, I.; Kaljurand, I.; Kütt, A.; Klamt, A.; Diedenhofen, M. *J. Comput. Chem.* **2009**, *30*, 799–810. (b) Kütt, A.; Leito, I.; Kaljurand, I.; Sooväli, L.; Vlasov, V. M.; Yagupolskii, L. M.; Koppel, I. A. *J. Org. Chem.* **2006**, *71*, 2829–2838.

(8) (a) Spitler, E. L.; Shirtcliff, L. D.; Haley, M. M. *J. Org. Chem.* **2007**, *72*, 86–96. (b) Resch-Genger, U.; Li, Y. Q.; Bricks, J. L.; Kharlanov, V.; Rettig, W. *J. Phys. Chem. A* **2006**, *110*, 10956–10971.

TABLE 1. Photophysical Data in CH_3CN

	abs λ_{max} (nm)	ε (M^{-1} cm^{-1})	em λ_{max} (nm)	Φ_F[a]	em λ_{max},[b] + acid (nm)	Φ_F,[b] + acid
5-H	295	30500	352	0.084	401	0.083
5-CH_3	297	36100	356	0.096	420	0.065
5-CF_3	317	33600	366	0.060	374	0.11
6-H	319, 271	19500, 18400	360	0.11	393	0.25
6-CH_3	321, 274	19500, 16200	357	0.084	410	0.10
6-CF_3	320, 275	18700, 19500	367	0.056	374	0.082
7	301	34400	359	0.046	359	0.043

[a]Referenced to 7-amino-4-methylcoumarin (Φ_F = 0.33 in CH_3OH). [b]Measured at the completion of titrations with CH_3SO_3H, CCl_3COOH, or CF_3COOH.

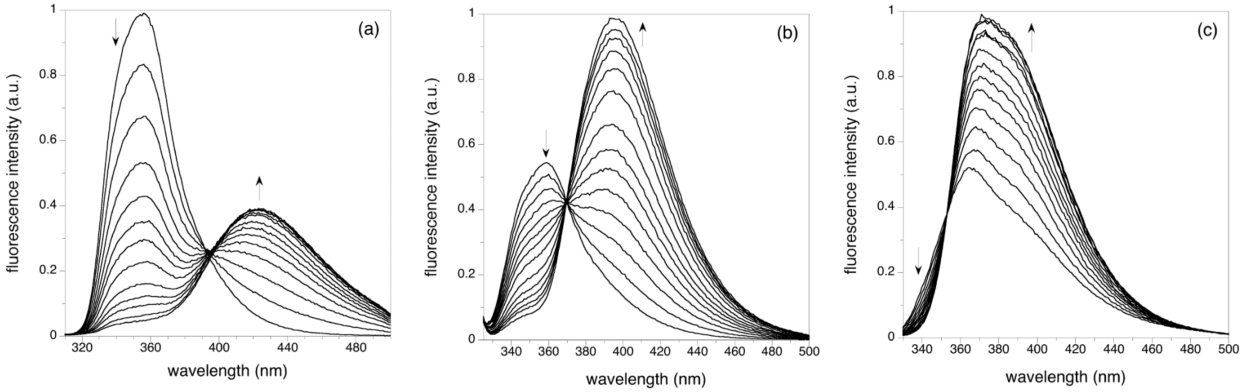

FIGURE 2. Emission spectra of selected sensors in CH_3CN during titration with CF_3COOH (0 → 1000 equiv): (a) **5-CH_3** (1.32×10^{-6} M), λ_{ex} = 300 nm; (b) **6-H** (1.56×10^{-6} M), λ_{ex} = 320 nm; and (c) **5-CF_3** (1.41×10^{-6} M), λ_{ex} = 320 nm.

With **6-H** and **6-CH_3** the red shifts are less pronounced. Protonation studies of fluorescent tetrakis(arylethynyl)benzenes have shown that electronic communication differs between pyridyl N atoms and arylethynyl linkers that lie ortho or meta to each other.[8a] Quantum yields for all three of the 6-isomers increase upon acidification; the most extreme case is shown in Figure 2b. Sensors **5-CF_3** (Figure 2c) and **6-CF_3** experience a red shift of less than 10 nm. Compound **7**, which lacks an intended protonation site, is unaffected by acidification.

Protonation of pyridine-containing fluorophores can give rise to new emission bands at longer wavelengths, by making internal charge transfer (ICT) from a donor to the heterocycle energetically favorable.[9] Frontier molecular orbitals for representative fluorophores **5-CH_3** and **5-CF_3** were visualized by using time-dependent DFT[10] in a solvent field corresponding to CH_3CN. In both of these hosts the HOMO and LUMO are uniformly delocalized over the urea−diarylacetylene π system, with electronic transition maxima calculated to appear at 328 and 338 nm, respectively. However, the next-highest MO for **5-CH_3** (LUMO+1) resides exclusively on the pyridine ring (Figure 3). As observed for other embedded-base fluorophores,[11] protonation should stabilize the localized orbital to a greater extent than the spatially dispersed HOMO or LUMO. This is borne out by the putative complex $H^+ \cdot$**5-CH_3**$\cdot CF_3COO^-$, in which H^+ and CF_3COO^- ions are bound at the pyridyl N atom and urea NH groups, respectively. Here, the pyridine-centered MO is predicted to lie below the delocalized one in energy, and emission from $H^+ \cdot$**5-CH_3**$\cdot CF_3COO^-$ is bathochromically shifted to 355 nm. In contrast, the calculated λ_{max} for trifluoromethyl-containing complex $H^+ \cdot$**5-CF_3**$\cdot CF_3COO^-$ (340 nm) is almost identical with that expected for the free base.

Fluorescence spectra of the six sensors were integrated from their respective isoemissive points to 500 nm during titrations with CCl_3COOH and CF_3COOH. The resultant F values increase by a factor of 4−6 for **5-H**/**CH_3** and **6-H**/**CH_3**, and approximately double for **5-CF_3** and **6-CF_3**. Normalized response curves (i.e., F/F_0 vs $[acid]_{total}$) are hyperbolic for all but **6-CF_3**, for which they have weak and distorted sigmoidal character (see the Supporting Information). Sensitivity is low. Addition of an approximately 1000-fold excess of each acid is required to achieve saturation. The 1:1 association constants[12,13] (Table 2) show that the sensors are not selective for trichloroacetic acid, even though it is significantly more ionized than CF_3COOH in acetonitrile. Indeed, the DFT-calculated binding energies for $H^+ \cdot$**5-H**$\cdot CCl_3COO^-$ and $H^+ \cdot$**5-H**$\cdot CF_3COO^-$ in an acetonitrile dielectric continuum, −9.3 and −9.6 kcal/mol, respectively,

(9) (a) Liu, Y.; Han, M.; Zhang, H.-Y.; Yang, L.-X.; Jiang, W. *Org. Lett.* **2008**, *13*, 2873–2876. (b) Pischel, U.; Heller, B. *New J. Chem.* **2008**, *32*, 395–400. (c) Kozhevnikov, D. N.; Shabunina, O. V.; Kopchuk, D. S.; Slepukhin, P. A.; Kozhevnikov, V. N. *Tetrahedron Lett.* **2006**, *47*, 7025–7029. (d) Ihmels, H.; Meiswinkel, A.; Mohrschladt, C. J.; Otto, D.; Waidelich, M.; Towler, M.; White, R.; Albrecht, M.; Schnurpfeil, A. *J. Org. Chem.* **2005**, *70*, 3929–3938.

(10) (a) Delley, B. *J. Chem. Phys.* **1990**, *92*, 508–517. (b) Delley, B. *J. Chem. Phys.* **2000**, *113*, 7756–7764. (c) Becke, A. D. *J. Chem. Phys.* **1988**, *88*, 1053–1062. (d) Tsuneda, T.; Hirao, K. *Chem. Phys. Lett.* **1997**, *268*, 510–520. (e) Listorti, A.; Esposti, A. D.; Kishore, R. S. K.; Kalsani, V.; Schmittel, M.; Armaroli, N. *J. Phys. Chem. A* **2007**, *111*, 7707–7718.

(11) (a) Zucchero, A. J.; McGrier, P. L.; Bunz, U. H. F. *Acc. Chem. Res.* **2010**, *43*, 397–408. (b) Zucchero, A. J.; Wilson, J. N.; Bunz, U. H. F. *J. Am. Chem. Soc.* **2006**, *128*, 11872–11881.

(12) (a) Hyperbolic fitting: Causey, C. P.; Allen, W. E. *J. Org. Chem.* **2002**, *67*, 5963–5968. (b) Sigmoidal fitting: Tian, Y.; Su, F.; Weber, W.; Nandakumar, V.; Shumway, B. R.; Jin, Y.; Zhou, X.; Holl, M. R.; Johnson, R. H.; Meldrum, D. R. *Biomaterials* **2010**, *31*, 7411–7422. (c) Connors, K. A. *Binding Constants*; Wiley: New York, 1987.

(13) Association constants derived from ratiometric treatment of the fluorescence data were unreasonably large. For a system that gives consistent K_{assoc} values from both direct and ratiometric fits, see: Baruah, M.; Qin, W.; Vallée, R. A. L.; Beljonne, D.; Rohand, T.; Dehaen, W.; Boens, N. *Org. Lett.* **2005**, *7*, 4377–4380.

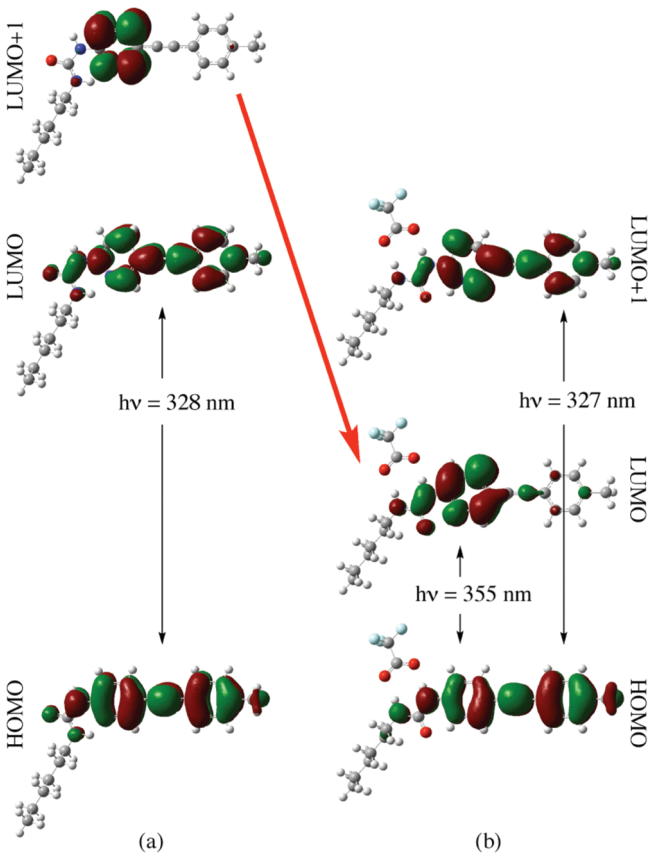

FIGURE 3. Calculated frontier molecular orbitals of **5-CH$_3$** (a) before and (b) after complexation with CF_3COOH.

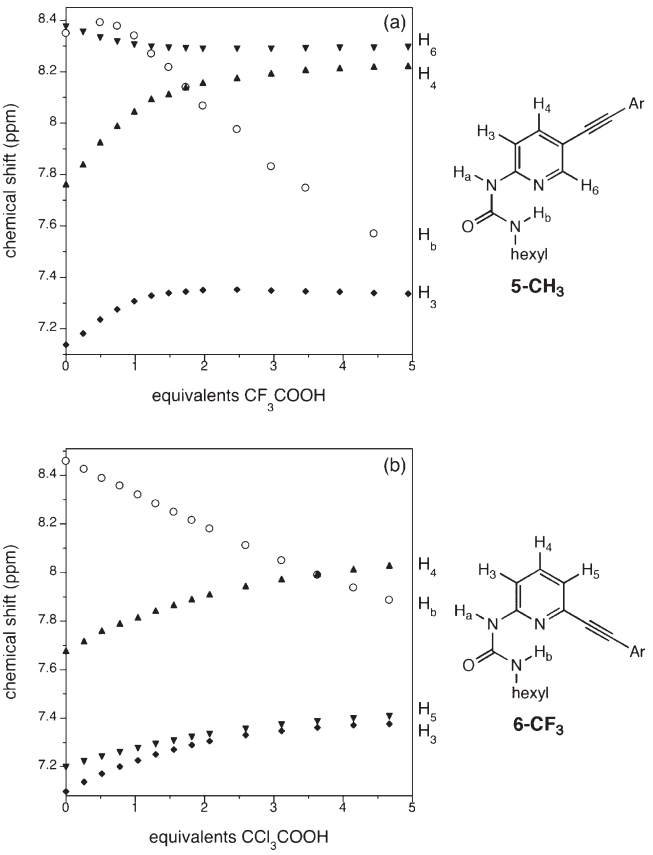

FIGURE 4. Chemical shifts of selected sensors in CD_3CN during titration with trihaloacetic acids: (a) **5-CH$_3$** (5.74×10^{-3} M) + CF_3COOH and (b) **6-CF$_3$** (5.88×10^{-3} M) + CCl_3COOH.

TABLE 2. Fluorescence Response of Sensors 5−6 to Increasing Concentrations of Acetic Acids in CH_3CN[a]

	CCl_3COOH	CF_3COOH	$CHCl_2COOH$	CH_3COOH
5-H	5000	3900	quenching	quenching
5-CH$_3$	4500	5200	quenching	quenching
5-CF$_3$	2300	2600	∼200[c]	quenching
6-H	600	800	∼200[c]	quenching
6-CH$_3$	1000	1900	630	quenching
6-CF$_3$	1100[b]	1000[b]	quenching	quenching

[a]Numerical values are averaged association constants (in M^{-1}) derived from at least two replicate experiments. Unless otherwise indicated, binding isotherms were fit to a hyperbolic function as described in the Experimental Section. [b]Sigmoidal plots of F/F_0 vs $\log[\text{acid}]_{\text{total}}$. [c]Negligible curvature in binding isotherms.

favor the acid with the more basic carboxylate ion. K_{assoc} values must reflect the composite thermodynamics of both *N*-protonation and hydrogen bonding to conjugate bases, so carboxylate binding makes a significant contribution to the overall stabilities of complexes.

Additional titrations were performed with CH_3COOH (pK_a in $CH_3CN = 23.51$) and $CHCl_2COOH$ (15.8[14]) to delineate the minimum acid strength necessary to "activate" **5**−**6**.[15] Acetic acid does not alter the position of the fluorescence band of any of the sensors. Integrated intensities, obtained over the entire emission range, decrease linearly with $[CH_3COOH]$. The average Stern−Volmer quenching constant (K_{SV}) with **5-H**/**CH$_3$**/**CF$_3$** is $46 \pm 4\ M^{-1}$.[16] An identical K_{SV} value ($44 \pm 1\ M^{-1}$) was found using the 6-isomers. Dichloroacetic acid causes fluorescence enhancement in **5-CF$_3$**, **6-H**, and **6-CH$_3$**, though only **6-CH$_3$** binds the acid strongly enough to display saturation behavior, and acts as a simple quencher toward the other fluorophores. Thus, the pK_a of this sensor class lies between about 13 and 16, in good agreement with the pK_a of 2-aminopyridine, 14.47.[17]

Proton NMR Response to Acids. ^{1}H NMR binding studies were performed in CD_3CN for **5-H**/**CH$_3$**/**CF$_3$** with CCl_3COOH and CF_3COOH. The chemical shifts from a typical titration of **5-CH$_3$** + trifluoroacetic acid are presented in Figure 4a. Only pyridyl proton H_4, which is more than three bonds removed from the expected sites of protonation and carboxylate recognition, moves in a smooth asymptotic manner. Both H_3 and H_6 subtly reverse direction at >1 equiv of acid, while the reaction of H-bonded urea proton H_b is more dramatic. Initially this resonance undergoes a small increase in δ indicative of more robust H-bonding, presumably to CF_3COO^-. At higher $[CF_3COOH]$ the

(14) Hayakawa, Y.; Iwase, T.; Nurminen, E. J.; Tsukamoto, M.; Kataoka, M. *Tetrahedron* **2005**, *61*, 2203–2209.

(15) In acetonitrile, **5-H** and **6-CH$_3$** do not display "off-on" fluorescence response toward CH_3COO^- or Cl^- (as tetrabutylammonium salts). Acetate ion acts as a quencher, while chloride causes no change in F or λ_{em}. For reviews of urea-based anion receptors, see: (a) Steed, J. W. *Chem. Soc. Rev.* **2010**, *39*, 3686–3699. (b) Li, A.-F.; Wang, J.-H.; Wang, F.; Jiang, Y.-B. *Chem. Soc. Rev.* **2010**, *39*, 3729–3745. (c) Gale, P. A. *Chem. Soc. Rev.* **2010**, *39*, 3746–3771. (d) Amedola, V.; Fabbrizzi, L.; Mosca, L. *Chem. Soc. Rev.* **2010**, *39*, 3889–3915.

(16) Sadowska, M.; Miller, E.; Wysocki, S.; Rodríguez-Muniz, G. M.; Costero, A. M.; Wandelt, B. *J. Lumin.* **2010**, *130*, 1085–1091.

(17) Kaljurand, I.; Kütt, A.; Sooväli, L.; Rodima, T.; Mäemets, V.; Leito, I.; Koppel, I. A. *J. Org. Chem.* **2005**, *70*, 1019–1028.

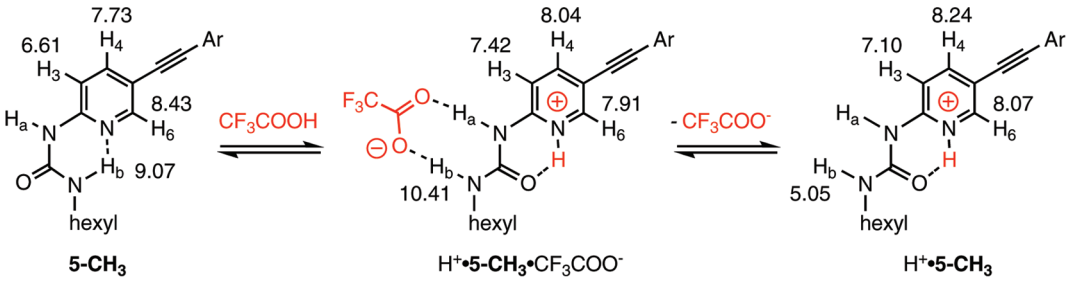

FIGURE 5. Calculated chemical shifts (ppm, in CH_3CN dielectric field) of **5-CH$_3$** and its proposed complexes with CF_3COOH.

shift of H_b decreases significantly. Addition of CCl_3COOH results in similar qualitative behavior. Maximum shifts of H_b are 0.05 ppm lower, on average, than those measured during titrations with CF_3COOH, reflecting the poorer H-bond acceptor ability of trichloroacetate. In every case the data from H_4 fit cleanly to a 1:1 stoichiometry model,[18] but with apparent binding constants that are an order of magnitude lower than ones derived from fluorescence experiments. Given the complex behavior of H_3, H_6, and H_b, the discrepancies likely arise from the presence of additional solution equilibria.[19] Attempts to describe the shifts of H_3 by including both 1:1 and 1:2 sensor/acid stoichiometries in the fitting routine brought the $K_{1:1}$ values more in line with those from fluorescence, but large errors in $K_{1:2}$ rendered the overall fits unreliable. Sensor self-association, which has been observed for other heterocyclic ureas in the NMR concentration regime,[1c] was determined to be a minor factor. Diluting a CD_3CN solution of **6-H** from 2.1×10^{-3} M to 9.0×10^{-5} M caused the ureido H_a signal to progress upfield by 0.03 ppm.

Simulated ^{1}H NMR spectra were generated for the lowest-energy DFT structures of **5-CH$_3$** and $H^+ \cdot$**5-CH$_3$**$\cdot CF_3COO^-$. The acid-binding mode at the center of Figure 5 correctly predicts the behavior of urea H_b at the outset of the titrations. This proton is calculated to become more deshielded as its intramolecular interaction with pyridine is replaced by an intermolecular one with trifluoroacetate (δ_{calc} = 9.07→10.41 ppm). Furthermore, the complex features downfield shifts in pyridyl H_3 and H_4, and an upfield change in H_6, as experimentally observed. Upon removing the bound CF_3COO^- guest, the computed shifts of cation $H^+ \cdot$**5-CH$_3$** follow the directional trends of the actual titrations at high [CF_3COOH]. Excess acid may facilitate decomplexation of carboxylate by allowing for formation of species like $CF_3COO^- \cdots (HOOCF_3)_n$, with favorable hard −hard acid−base character.[20]

The sensor/acid combinations that produced anomalous sigmoidal fluorescence curves were also examined by NMR. Treatment of **6-CF$_3$** with CCl_3COOH or CF_3COOH causes all three pyridyl protons to shift downfield in a manner consistent with protonation (Figure 4b), although natural population analysis of pyridyl N atomic charges suggests **6-CF$_3$** is less basic than other sensors. Urea H_b does not experience an increase in chemical shift early in the titrations, but instead tracks uniformly upfield. Assuming that a carboxylate binding model akin to that shown at the center of Figure 5 is operative for this system—examination of the electrostatic potential map of $H^+ \cdot$**6-CF$_3$** failed to identify obvious alternative sites for recognition of CX_3COO^-—then the H-bonding from H_b to $CXCOO^-$ must be weak. Notably, sigmoidal fluorescence behavior is elicited from all six sensors by CH_3SO_3H, the conjugate base of which is a significantly poorer hydrogen bond acceptor than the trifluoroacetates. The pK_a of methanesulfonic acid is 9.97 in CH_3CN, and its tetrahedral sulfonate is not an optimal steric match to the planar H-bonding array presented by a urea group. *F* values of **5**−**6** increase until 10−20 equiv of CH_3SO_3H are present, confirming that the fluorophores are protonated by this acid. Normalized response curves have asymmetrical "S"-shapes, which resolve into sigmoidal outputs typical of acid/base titrations by plotting F/F_0 as a function of log[CH_3SO_3H]$_{total}$ (see the Supporting Information). An NMR study of **5-CF$_3$** showed only upfield shifts in H_b during acidification with CH_3SO_3H in acetonitrile. Therefore, it appears that sensor protonation and unfolding can occur without concomitant binding of the conjugate base at the urea moiety.

Conclusions

Fluorescence output of the present pyridyl urea-based receptors is intimately linked to the strength of the organic acids added to them, though members of this class do not report solely on [H^+]. Trichloroacetic and trifluoroacetic acids, at equivalent concentrations, induce similar "off-on" emission enhancements despite their pK_a difference of nearly 2 orders of magnitude. The relatively greater basicity of CF_3COO^- leads to tighter H-bonding at the urea NH groups, compensating for the parent acid's lower degree of ionization, and driving complexation.

Experimental Section

1-Hexyl-3-(5-iodopyridin-2-yl)urea (2). A round-bottomed flask containing 15 mL of dry THF was charged with 2-amino-5-iodopyridine (1.14 g, 5.18 mmol) and hexyl isocyanate (0.66 g, 5.2 mmol). Under N_2, the mixture was heated to reflux with stirring for 72 h. The solution was allowed to cool to rt and the THF was removed by rotary evaporation. The resulting yellow oil was dissolved in CH_2Cl_2 and washed with 5% HCl then saturated $NaHCO_3$. The organic layer was dried over Na_2SO_4, filtered, and evaporated to afford 1.39 g (77%) of **2** as a cream-colored solid. This material was used in the subsequent step without further purification. Mp 94−96 °C; ^{1}H NMR ($CDCl_3$) δ 0.90 (t, 3H), 1.3−1.7 (m, 8H), 3.36 (q, 2H), 6.74 (d, 1H), 7.80 (dd, 1H), 8.34 (s, 1H), 9.01 (br s, 1H), 9.11 (s, 1H); ^{13}C NMR ($CDCl_3$) δ 14.0, 22.6, 26.6, 30.0, 31.5, 39.9, 81.5, 114.2, 145.9, 151.8, 152.6, 155.9; HRMS (ESI) calcd for $C_{12}H_{19}IN_3O$ $(M + H)^+$ 348.0567, found 348.0520.

1-(6-Bromopyridin-2-yl)-3-hexylurea (3). The procedure for **2** was followed, using 0.76 g (4.4 mmol) of 2-amino-6-bromopyridine and 0.57 g (4.5 mmol) of hexyl isocyanate. After workup, 1.12 g (85%) of **3** was obtained as light yellow crystals. This material was used in the subsequent step without further purification. Mp 78−80 °C;

(18) Hynes, M. J. *J. Chem. Soc., Dalton Trans.* **1993**, 311–312.
(19) dos Santos, C. M. G.; McCabe, T.; Watson, G. W.; Kruger, P. E.; Gunnlaugsson, T. *J. Org. Chem.* **2008**, *73*, 9235–9244.
(20) Pérez, P.; Toro-Labbé, A.; Contreras, R. *J. Phys. Chem. A* **2000**, *104*, 5882–5887.

^{1}H NMR ($CDCl_3$) δ 0.90 (t, 3H), 1.3−1.7 (m, 8H), 3.39 (q, 2H), 6.89 (d, 1H), 7.02 (dd, 1H), 7.42 (t, 1H), 8.84 (br s, 1H), 9.48 (s, 1H); ^{13}C NMR ($CDCl_3$) δ 14.1, 22.6, 26.7, 29.6, 31.6, 40.0, 110.3, 120.0, 137.9, 140.1, 153.5, 155.5; HRMS (ESI) calcd for $C_{12}H_{19}BrN_3O$ $(M + H)^+$ 300.0706, found 300.0800.

1-Hexyl-3-(4-iodophenyl)urea (4). The procedure for **2** was followed, using 1.97 g (8.99 mmol) of 4-iodoaniline and 1.37 g (10.8 mmol) of hexyl isocyanate in 30 mL of THF. After workup, 3.09 g (99%) of **4** was obtained as an off-white solid. Recrystallization from absolute ethanol provided an analytical sample as colorless plates. Mp 166−168 °C; ^{1}H NMR ($CDCl_3$) δ 0.89 (t, 3H), 1.2−1.4 (m, 6H), 1.52 (m, 2H), 3.24 (q, 2H), 4.55 (br s, 1H), 6.13 (s, 1H), 7.10 (d, 2H), 7.60 (d, 2H); ^{13}C NMR (DMSO-d_6) δ 13.9, 22.0, 26.0, 29.6, 31.0, 83.3, 119.8, 137.1, 140.5, 154.9; HRMS (ESI) calcd for $C_{13}H_{20}IN_2O$ $(M + H)^+$ 347.0615, found 347.0633.

1-Hexyl-3-(5-(phenylethynyl)pyridin-2-yl)urea (5-H). A pressure tube containing 10 mL of acetonitrile and a stir bar was charged with **2** (0.69 g, 2.0 mmol), phenylacetylene (0.22 g, 2.1 mmol), and piperidine (0.86 g, 10 mmol). With stirring, N_2 was bubbled into the suspension for 5 min, followed by the addition of 0.047 g (0.040 mmol) of tetrakis(triphenylphosphine)palladium(0). The pressure tube was immediately sealed and lowered into an oil bath that was preheated to 85 °C. The mixture clarified over several minutes. After 90 min, stirring was stopped and the tube was allowed to cool to rt for 18 h in the dark. During this time, the mixture deposited a cream colored precipitate. The solid was collected by filtration, washed with ice-cold CH_3CN, and dried under vacuum to afford 0.58 g (89%) of **5-H** as a lustrous, off-white solid. Mp 131−133 °C; ^{1}H NMR ($CDCl_3$) δ 0.91 (t, 3H), 1.3−1.5 (m, 4H), 1.5−1.7 (m, 4H), 3.39 (q, 2H), 6.73 (d, 1H), 7.36 (m, 3H), 7.52 (m, 2H), 7.70 (dd, 1H), 7.86 (s, 1H), 8.35 (d, 1H), 9.17 (br s, 1H); ^{13}C NMR ($CDCl_3$) δ 14.0, 22.6, 26.7, 29.8, 31.5, 40.0, 85.9, 91.2, 111.2, 113.1, 122.8, 128.4, 128.5, 131.5, 140.7, 149.2, 152.1, 155.3; FTIR (ATR, solid) ν 3342, 3224, 3134, 1667 cm^{-1}; UV/vis (CH_3CN) λ_{max} (ε, M^{-1} cm^{-1}) 295 (30500); HRMS (ESI) calcd for $C_{20}H_{24}N_3O$ $(M + H)^+$ 322.1919, found 322.1790. Anal. Calcd for $C_{20}H_{23}N_3O$: C, 74.74; H, 7.21; N, 13.07. Found: C, 74.62; H, 7.12; N, 12.80.

1-Hexyl-3-(5-(*p*-tolylethynyl)pyridin-2-yl)urea (5-CH$_3$). The procedure for **5-H** was followed, using 0.512 g (1.47 mmol) of **2**, 0.171 g (1.47 mmol) of *p*-tolylacetylene, 0.65 g (7.6 mmol) of piperidine, and 0.034 g (0.030 mmol) of $Pd(PPh_3)_4$ catalyst. The reaction mixture clarified over several minutes and after 1 h a precipitate had formed. Stirring was stopped at 90 min and the tube was allowed to cool to rt for 18 h in the dark. The precipitate was collected by filtration and washed with ice-cold CH_3CN. Drying under vacuum gave 0.39 g (80%) of **5-CH$_3$** as a white solid. Mp 145−147 °C; ^{1}H NMR ($CDCl_3$) δ 0.90 (t, 3H), 1.2−1.5 (m, 6H), 1.60 (m, 2H), 2.38 (s, 3H), 3.38 (q, 2H), 6.70 (d, 1H), 7.17 (d, 2H), 7.41 (d, 2H), 7.67 (s, 1H), 7.68 (d, 1H), 8.34 (s, 1H), 9.17 (br s, 1H); ^{13}C NMR ($CDCl_3$) δ 14.1, 21.5, 22.6, 26.7, 29.9, 31.5, 40.0, 85.2, 98.6, 111.1, 113.4, 119.7, 129.2, 131.4, 138.7, 140.7, 149.2, 152.0, 155.2; FTIR (ATR, solid) ν 3352, 3223, 3130, 1670 cm^{-1}; UV/vis (CH_3CN) λ_{max} (ε, M^{-1} cm^{-1}) 297 (36100); HRMS (ESI) calcd for $C_{21}H_{26}N_3O$ $(M + H)^+$ 336.2076, found 336.2094. Anal. Calcd for $C_{21}H_{25}N_3O$: C, 75.19; H, 7.51; N, 12.53. Found: C, 75.17; H, 7.43; N, 12.39.

1-Hexyl-3-(5-((4-(trifluoromethyl)phenyl)ethynyl)pyridin-2-yl)-urea (5-CF$_3$). The procedure for **5-H** was followed, using 0.63 g (1.8 mmol) of **2**, 0.32 g (1.9 mmol) of 1-ethynyl-4-(trifluoromethyl)-benzene, 0.77 g (9.0 mmol) of piperidine, and 0.042 g (0.036 mmol) of $Pd(PPh_3)_4$ catalyst. After 90 min, stirring was stopped and the tube was allowed to cool to rt for 18 h in the dark. The yellow precipitate was collected via filtration, washed with ice-cold CH_3CN, and dried under vacuum to give 0.55 g (79%) of **5-CF$_3$** as a fluffy, off-white solid. Mp 160−162 °C; ^{1}H NMR ($CDCl_3$) δ 0.91 (t, 3H), 1.2−1.5 (m, 6H), 1.63 (m, 2H), 3.40 (q, 2H), 6.89 (d, 1H), 7.62 (s, 4H), 7.73 (dd, 1H), 8.36 (s, 1H), 9.08 (s, 1H), 9.22 (br s, 1H); ^{13}C NMR ($CDCl_3$) δ 14.1, 22.6, 26.7, 29.9, 31.5, 40.0, 88.5, 89.7, 111.7, 112.2, 122.1, 125.4, 126.7, 131.7, 140.7, 149.5, 152.9, 155.8; FTIR (ATR, solid) ν 3338, 3224, 3133, 1671 cm^{-1}; UV/vis (CH_3CN) λ_{max} (ε, M^{-1} cm^{-1}) 317 (33600). Anal. Calcd for $C_{21}H_{22}F_3N_3O$: C, 64.77; H, 5.69; N, 10.79. Found: C, 64.72; H, 5.64; N, 10.71.

1-Hexyl-3-(6-(phenylethynyl)pyridin-2-yl)urea (6-H). The procedure for **5-H** was followed, using 0.60 g (2.0 mmol) of **3**. After 6 h, stirring was stopped and the orange solution was allowed to cool to rt for 18 h in the dark. The precipitated product was collected by filtration, washed with ice-cold CH_3CN, and dried under vacuum to yield 0.34 g (53%) of **6-H** as yellow plates. Mp 153−154 °C; ^{1}H NMR ($CDCl_3$) δ 0.83 (t, 3H), 1.3−1.5 (m, 4H), 1.47 (m, 2H), 1.66 (m, 2H), 3.42 (q, 2H), 6.81 (d, 1H), 7.11 (d, 1H), 7.39 (m, 3H), 7.55 (m, 3H), 8.31 (s, 1H), 9.30 (br s, 1H); ^{13}C NMR ($CDCl_3$) δ 14.0, 22.6, 26.7, 29.6, 31.6, 39.9, 88.3, 89.0, 111.6, 120.3, 122.2, 128.4, 129.0, 131.9, 138.2, 139.5, 153.4, 155.8; FTIR (ATR, solid) ν 3358 (wk), 3214, 3122, 1677 cm^{-1}; UV/vis (CH_3CN) λ_{max} (ε, M^{-1} cm^{-1}) 271 (18400), 319 (19500). Anal. Cacld for $C_{20}H_{23}N_3O$: C, 74.74; H, 7.21; N 13.07. Found: C, 74.77; H, 7.21; N, 12.95.

1-Hexyl-3-(6-(*p*-tolylethynyl)pyridin-2-yl)urea (6-CH$_3$). The procedure for **5-H** was followed, using 0.541 g (1.81 mmol) of **3** and 0.211 g (1.82 mmol) of *p*-tolylacetylene. The reaction clarified after several minutes. After 6 h, stirring was stopped and the tube was allowed to cool to rt for 18 h in the dark. The yellow solution deposited a precipitate that was collected via filtration and washed with ice-cold CH_3CN. Drying under vacuum afforded 0.37 g (60%) of **6-CH$_3$** as a pale yellow solid. Mp 145−146 °C; ^{1}H NMR ($CDCl_3$) δ 0.87 (t, 3H), 1.30 (m, 4H), 1.44 (m, 2H), 1.65 (m, 2H), 2.39 (s, 3H), 3.42 (q, 2H), 6.88 (d, 1H), 7.08 (dd, 1H), 7.18 (d, 2H), 7.44 (d, 2H),7.53 (t, 1 H), 8.94 (s, 1H), 9.32 (br s, 1H); ^{13}C NMR ($CDCl_3$) δ 14.1, 21.6, 22.6, 26.8, 29.7, 31.6, 39.9, 87.9, 89.3, 111.6, 119.1, 120.2, 129.2, 131.8, 138.2, 139.3, 139.6, 153.5, 156.1; FTIR (ATR, solid) ν 3364 (wk), 3218, 3110, 1679 cm^{-1}; UV/vis (CH_3CN) λ_{max} (ε, M^{-1} cm^{-1}) 274 (16200), 321 (19500); HRMS (ESI) calcd for $C_{21}H_{26}N_3O$ $(M + H)^+$ 336.2076, found 336.2006. Anal. Calcd for $C_{21}H_{25}N_3O$: C, 75.19; H, 7.51; N, 12.53. Found: C, 74.95; H, 7.47; N, 12.68.

1-Hexyl-3-(6-((4-(trifluoromethyl)phenyl)ethynyl)pyridin-2-yl)-urea (6-CF$_3$). The procedure for **5-H** was followed, using 0.60 g (2.0 mmol) of **3** and 0.37 g (2.2 mmol) of 1-ethynyl-4-(trifluoromethyl)benzene. After 6 h, stirring was stopped and the mixture was allowed to cool to rt for 18 h in the dark. The precipitate was collected via filtration, washed with ice-cold CH_3CN, and dried under vacuum to give 0.44 g (56%) of **6-CF$_3$** as white needles. Mp 166−167 °C; ^{1}H NMR ($CDCl_3$) δ 0.83 (t, 3H), 1.30 (m, 4H), 1.47 (m, 2H), 1.63 (m, 2H), 3.42 (q, 2H), 6.84 (d, 1H), 7.14 (d, 1H), 7.61 (m, 5H), 8.36 (s, 1H), 9.23 (br s, 1H); ^{13}C NMR ($CDCl_3$) δ 14.0, 22.6, 26.8, 29.6, 31.6, 39.9, 87.3, 90.4, 112.1, 120.6, 125.4, 132.2, 138.3, 138.9, 153.4, 155.6; FTIR (ATR, solid) ν 3366 (wk), 3220, 3118, 1682 cm^{-1}; UV/vis (CH_3CN) λ_{max} (ε, M^{-1} cm^{-1}) 275 (19500), 320 (18700). Anal. Calcd for $C_{21}H_{22}F_3N_3O \cdot 0.25(H_2O)$: C, 64.03; H, 5.76; N, 10.67. Found: C, 64.27; H, 5.53; N, 10.67.

1-Hexyl-3-(4-(phenylethynyl)phenyl)urea (7). The procedure for **5-H** was followed, using 0.70 g (2.0 mmol) of **4**. Stirring was stopped after 90 min and the tube was allowed to cool to rt for 18 h in the dark. The precipitate was collected by filtration, washed with ice-cold CH_3CN, and dried under vacuum to afford 0.46 g (71%) of **7** as yellow needles. Mp 134−142 °C dec; ^{1}H NMR ($CDCl_3$) δ 0.89 (t, 3H), 1.2−1.4 (m, 6H), 1.52 (m, 2H), 3.25 (q, 2H), 4.75 (br s, 1H), 6.43 (s, 1H), 7.32 (t, 5H), 7.46 (d, 2H), 7.51 (dd, 2H); ^{13}C NMR ($CDCl_3$) δ 14.0, 22.6, 26.6, 30.0, 31.5, 40.6, 88.8, 89.2, 118.0, 119.9, 123.4, 128.1, 128.3, 131.5, 132.6, 138.8, 155.1; UV/vis (CH_3CN) λ_{max} (ε, M^{-1} cm^{-1}) 301 (34400). Anal. Calcd for $C_{21}H_{24}N_2O$: C, 78.71; H, 7.55; N, 8.74. Found: C, 78.80; H, 7.51; N, 8.64.

Fluorescence Titrations. Sensors **5**−**7** were dissolved in spectrophotometric grade CH_3CN to concentrations of 1.5×10^{-6}−2.0×10^{-6} M, and an electronic absorption spectrum was acquired for each to ensure that the absorbance was less than 0.05. A 3.0 mL sample was transferred to a quartz cuvette containing a small magnetic stir bar. The solution was excited near its predetermined

λ_{max} (i.e., 300 or 320 nm), and an emission spectrum was recorded. Aliquots of organic acid solutions, prepared in CH_3CN to be up to 300 times more concentrated than that of the sensor solution, were added to the cuvette and the contents were stirred for 1 min before being scanned. This process was repeated until the fluorescence spectra ceased to evolve. For sensor/acid combinations that displayed fluorescence enhancement, the integrated emission intensity (F) was computed from the isoemissive point to 500 nm for each spectrum. Data were normalized by dividing each F value by F_0, then were plotted as a function of $[acid]_{total}$. Derivation of binding constants varied depending upon the appearance of the normalized response curves so obtained. Hyperbolic data sets were fit to the equation $F/F_0 = \{1 + (k_{complex}/k_{sensor})K_{assoc}[acid]_{total}\}/(1 + K_{assoc}[acid]_{total})$, as previously described.[12a] Sigmoidal curves were fit to $F/F_0 = 1 + \{\{(F_{max}/F_0) - 1\}/\{1 + (K_{assoc}[acid]_{total})^p\}\}$, where F_{max} is the integrated intensity at highest acid concentration, p is a slope parameter, and $[acid]_{total}$ is placed on a logarithmic scale.[12b] During iterative fitting, values of K_{assoc} and p were allowed to vary freely. For cases where weak binding was apparent (little or no curvature in binding isotherms), values were obtained by linear fitting to $F/F_0 = K_{assoc}[CHCl_2COOH]_{total}$. For acetic acid or dichloroacetic acid acting as a simple quencher, Stern−Volmer constants were calculated from the best fit line to the equation $F_0/F = 1 + K_{SV}[acid]_{total}$.

^{1}H NMR Titrations. With sonication and gentle heating, sensors were dissolved in CD_3CN to concentrations of 0.0056−0.0060 M. A 1.00 mL sample was transferred to an NMR tube. Aliquots of acid solutions, prepared to be ∼30× more concentrated than that of the host, were injected into the tube. After each addition the tube was capped and inverted several times, and a proton NMR spectrum was acquired. This process was repeated while monitoring the chemical shift of the pyridyl and urea protons until at least 5 equiv of acid were present in the tube. Association constants were calculated by using the nonlinear fitting program WinEQNMR.[18]

Computational Modeling. Routine geometry optimizations were run through the numerical DFT program DMol3 and employed the Becke-Tsuneda-Hirao gradient-corrected exchange-correlation functional and a double-numerical plus polarization basis set.[10] NMR chemical shifts and excitation/emission energies were calculated by using the GIAO and time-dependent density-functional theory (TDDFT) methods, respectively, as implemented in Gaussian 09. In both cases, molecular geometries were optimized at the same level of theory in which the properties were evaluated: B3LYP/6-31G** and B3LYP/tzvp for the NMR and TDDFT calculations, respectively, performed in the presence of a CPCM reaction field with the dielectric equal to that of acetonitrile.

Acknowledgment. W.E.A. thanks the ECU Division of Research and Graduate Studies for a Research Development Award. A.L.S. thanks the ECU CACS and NSF (CNS-0619285). L.M.J. was supported by a Burroughs-Wellcome Fellowship for 2008−2009. Purchase of NMR and mass spectrometers was made possible by the NSF (CRIF-0077988 and MRI-0521228, respectively).

Supporting Information Available: ^{1}H/^{13}C NMR spectra for all new compounds, crystallographic details, representative titration curves from fluorescence and ^{1}H NMR, and atomic coordinates of DFT-calculated structures. This material is available free of charge via the Internet at http://pubs.acs.org.